

Gas Shear Layers and Wakes Without And With Different Density Stratifications

Ralf Kapulla, Luke Ryan, Camille Zimmer

Paul Scherrer Institut, 5232 Villigen, Switzerland

Abstract

Shear layer and wake flows are examples of so called ‘building block’ flows for hydrodynamics which have been studied for a long time. The HOMER test facility at the Paul Scherrer Institute in Switzerland is dedicated to study such fundamental mixing processes in the presence of different density stratifications and shear strengths. The HOMER facility consists of a horizontal mixing section fed by two vertically stacked initially separated gas streams which interact downstream of a splitter plate. The strength of the density stratification was controlled by changing the gas species in each of the streams. The gas species used in the upper stream was altered between air, a helium-nitrogen mixture and pure helium while only air was used in the lower stream. In order to adjust the shear strength from isokinetic conditions (wake flow formed behind the splitter plate) to weak shear flow, independent velocity control of each stream was applied and experiments were conducted at two bulk velocities in order to observe any Reynolds number effects on the developing flow fields. Measurements were made using 2D Particle Image Velocimetry with the light sheet located in the center of the cross-section of the channel. For the unstratified experiments, first shear layer results demonstrate the deflection of the developing flow field towards the low speed side while the flow field remains symmetric with respect to the test section top and bottom wall for the isokinetic case. The signature of the vortex chain developing past the splitter plate was made visible with cross-correlation maps and characteristic wavelengths λ_n and corresponding frequencies f_n of the vortices were deduced from these maps for all stratification strengths. The theoretical proportionality between the frequency and the mean velocity $f_n \sim \bar{u}_m^{3/2}$ was confirmed by all of the experiments except for the helium test cases at low velocities.

Keywords: shear layer, wake flow, density stratification.

1 Introduction

Mixing of fluids is usually associated with velocity shear; the vast majority of mixing layer experiments is thus conducted for shear layers. While less common, the study of shear free mixing is also of crucial importance in the exploration of mixing phenomena; examples of shear free mixing experiments include isokinetic mixing layers and “mixing box” experiments. Unstratified cases are vital as reference experiments to contrast the strength of the suppression of the mixing zone growth for the stratified experiments. Whereas it may appear that a stratified shear layer is completely dominated by the development of Kelvin-Helmholtz instabilities, various results of past growth law studies (Bell and Metha (1990); Browand and Latigo (1978); Brown and Roshko (1974); Mehta and Westphal (1986)) indicate that mixing layer development is also considerably influenced by the “history” of the two streams before they interact. For example, the amount of free stream small scale turbulence generated by grids located upstream of the splitter plate tip appeared to have a significant effect on the downstream flow interactions. This finding re-focused the interest of the research toward isokinetic mixing layers as a way to isolate these aspects and study them separately from those observations induced by shear effects. Regardless of this new interest there is still a very limited amount of available literature studying shear free mixing (Bidokhti and Britter (2002); McGrath et al. (1997); Veeravalli and Warhaft (1990); Yoon and Warhaft (1990)) when compared with the literature available on shear layers. For shear free (isokinetic and mixing box) mixing experiments the interaction process between the stratification and the turbulence is not well understood from a fundamental point of view. There is no consensus on the dominating mixing mechanism; some mechanisms proposed in the literature include engulfment (McGrath et al. (1997)), generation of waves and their breaking (Fernando and Long (1985); Mory (1991)), eddy impingement (Dahm et al. (1989); Linden (1975)), and the radiation of turbulence from the high turbulence side through the interface to the low turbulence side (Fernando (1991)).

The majority of stratified mixing layer experiments were conducted at moderate density differences. These density differences may be obtained by applying either different temperatures (thermal stratification) (Tavoularis and Corrsin (1981); Veeravalli and Warhaft (1990)) or different compositions (species stratification) (Bidokhti and Britter (2002); Koochesfahani and Dimotakis (1986); Rohr et al. (1988)) to the two streams. Some experimentalists choose to conduct similar tests using both to compare the added effects of a change in species, such as the potential effect of a different diffusivity, on the mixing process. Literature on mixing in the presence of high density differences is surprisingly scarce. There are only a few references outlining past shear layer experiments at high density differences (Bogdanoff (1984); Brown and Roshko (1974); Dimotakis (1986); Hill and Nicholson (1964); Johnson (1971); Konrad (1977)) and no examples of isokinetic experiments at high density differences were located. With an increasing demand for numerical prediction of highly density stratified flows, there exists a continued need for experimental data from high density difference experiments to develop, improve, and ultimately validate these codes.

2 Experiment

The experimental facility used for this project consists of an open GAs M_Ixing L_Oop (GAMILO) supplying two parallel gas flows of independent densities and velocities to a H_OriZontal M_Ixing E_Xperiment in a R_Ectangular channel (HOMER). The HOMER facility is a rectangular channel test section comprising of a flow conditioning inlet, a measurement section, and an exhaust system. A simplified schematic of HOMER is given in Figure 1. The coordinate system was placed at the middle of the splitter plate tip; the downstream distance is depicted by x , the crosswise direction by y and the spanwise direction by z .

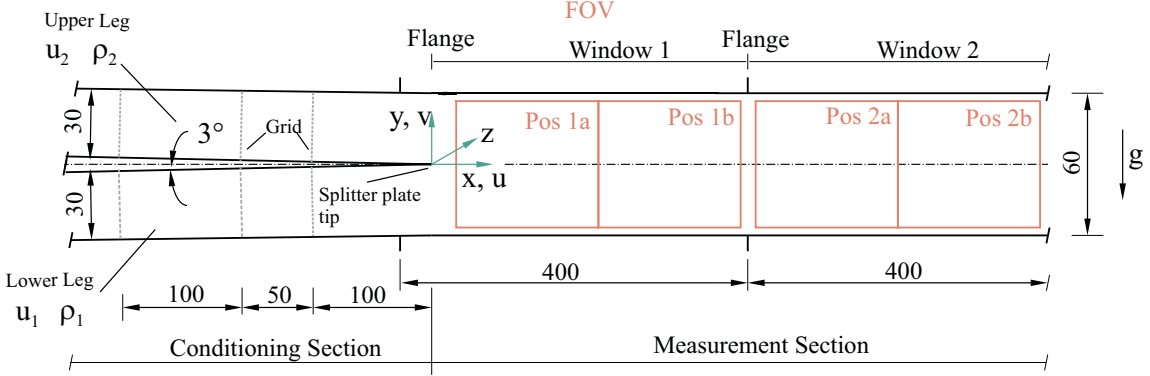


Figure 1: *Simplified schematic of the HOMER facility with conditioning and measurement sections. The main dimensions are given in mm.*

At the inlet to the HOMER facility, two gas streams are fed into two separated flow conditioning channels (each with a cross section of 30 mm by 60 mm) equipped with honeycombs (not shown) and grids. The purpose of the honeycombs is to remove any possible rotational components introduced into the flow by the gas supply loop. The purpose of the grids is to reduce the boundary layers, thus establishing an inlet profile which is as flat and even as possible. The final two grids are located at $x = -100\text{ mm}$ and $x = -150\text{ mm}$ upstream of the splitter plate tip, as shown in Figure 1. At the end of the conditioning section, the two flows meet at the tip of the splitter plate, which is angled at 3 degrees. Past the tip of the splitter plate, the measurement section begins as the two gas streams merge and interact to form the mixing zone. This section has a cross section of 60 mm by 60 mm . To measure the velocity field, Particle Image Velocimetry (PIV) measurements were taken through two consecutive glass windows. Measurements were taken between $15 \leq x \leq 340\text{ mm}$ in the first window and $475 \leq x \leq 820\text{ mm}$ in the second window. Both windows allow for measurements to be taken between $-25 \leq y \leq 25\text{ mm}$ in the vertical direction. The hardware was comprised of a *Litron NanoL* laser with nominal 200 mJ and a *PCO 1600* camera having a resolution of $1600 \times 1200\text{ pixels}^2$. For each Field of View (FOV) (Position 1a, 1b, 2a, and 2b in Figure 1) we conduct one PIV recording consisting of $N = 1024$ double images recorded with a frequency of $f = 15\text{ Hz}$. For the PIV analysis with DaVis 8.1 the instantaneous velocity fields were then calculated using a multi-pass approach with an initial interrogation window size of $64 \times 64\text{ pixels}^2$ and a

Exp. No.	Media	ν_1 m^2/s $\cdot 10^{-5}$	ν_2 m^2/s $\cdot 10^{-5}$	ρ_1 kg/m^3	ρ_2 kg/m^3	ρ_m kg/m^3	$\Delta\rho$ kg/m^3	a –	A –
N075-N080	Air-Air	1.582	1.582	1.169	1.169	1.17	0.00	1.00	0.00
N082-N086	Air-Mix	1.582	3.817	1.169	0.565	0.87	0.60	0.48	0.35
N087-N092	Air-He	1.582	12.30	1.169	0.161	0.67	1.01	0.14	0.76

Table 1: *Experimental numbers (N075 to N092) together with the gas species used and physical properties.*

final interrogation window size of 16×16 *pixels*² with 50% overlap. After calibration this results in an effective spatial resolution of 1.12×1.12 *mm*².

The present experiments focus on three parameters (i) the mean velocity $\bar{u}_m = (\bar{u}_1 + \bar{u}_2)/2$ of the flow, (ii) the shear strength between the two streams depicted by $\Delta\bar{u} = \bar{u}_1 - \bar{u}_2$, $r = \bar{u}_2/\bar{u}_1$ and $R = (\bar{u}_1 - \bar{u}_2)/(\bar{u}_1 + \bar{u}_2)$ and (iii) the stratification strength characterized by $\Delta\rho = \rho_1 - \rho_2$, $a = \rho_1/\rho_2$ and $A = (\rho_1 - \rho_2)/(\rho_1 + \rho_2)$. For $R = 0$ the flow reduces to a wake and for $R = 1$ only one stream is present similar to the initial reion of a jet. The strength of the density stratification was controlled by changing the gas species in each of the streams. The gas species used in the upper stream (index 2) was altered between air, a helium-nitrogen mixture and pure helium while only air was used in the lower stream (index 1). Additionally, to indicate the flow state – laminar versus turbulent – in the two channels of the conditioning section, the half channel Reynolds numbers $Re_{hc1(2)} = (\bar{u}_{1(2)} \cdot d_h)/\nu$ were calculated, see Tables 1 and 2.

3 Results

The experimental conditions for the experiments considered here can be found in Table 2. It is noted in Table 2 that for the Air-Mix experiments the high shear cases and for the Air-He experiments the isokinetic case for lowest velocity are missing. The three different stratification strengths are depicted in the table by ‘Air-Air’, ‘Air-Mix’ for the experiments with air in the lower and a nitrogen-helium mixture in the upper stream and ‘Air-He’ for the experiments with air in the lower and pure helium in the upper stream. The two different mean velocities are $\bar{u}_m \approx 3$ and $\bar{u}_m \approx 5.3$ *m/s*.

For the sake of brevity, a visual summary of the results is presented only for the air-air mixing experiments N075 and N077 (Figures 2 and 3), which are the low-velocity isokinetic and shear mixing cases, respectively. The mean velocity \bar{u} and velocity fluctuation $(\overline{u'u'})^{0.5}$ are shown on the top and bottom of each figure, respectively. In the isokinetic case (Figure 2), the velocity deficit past the splitter plate tip is caused by the merging of the boundary layers developing on the top and bottom wall of the splitter plate. This deficit is most pronounced in the centre of the wake, which is narrow in shape in the early stages of mixing. Gradually with downstream distance, the velocity deficit is filled up, the wake broadens and there is less of a velocity differential between

Exp. No.	Media	\bar{u}_1 m/s	\bar{u}_2 m/s	\bar{u}_m m/s	$\Delta\bar{u}$ m/s	r -	R † -	Re_{hc1} †† -	Re_{hc2} -
N075	Air-Air	2.954	2.959	2.957	-0.005	1.00	0.00	7500	7500
N076	Air-Air	3.073	2.883	2.978	0.190	0.94	0.03	7800	7300
N077	Air-Air	3.165	2.771	2.968	0.394	0.88	0.07	8000	7000
N078	Air-Air	5.234	5.274	5.254	-0.040	1.01	0.00	13000	13000
N079	Air-Air	5.423	5.105	5.264	0.318	0.94	0.03	13700	12900
N080	Air-Air	5.591	4.925	5.258	0.666	0.88	0.06	14100	12500
N085	Air-Mix	3.063	3.004	3.034	0.059	0.98	0.01	7700	3200
N086	Air-Mix	3.174	2.887	3.031	0.287	0.91	0.05	8000	3000
-	Air-Mix	-	-	-	-	-	-	-	-
N082	Air-Mix	5.408	5.288	5.348	0.120	0.98	0.01	13700	5500
N083	Air-Mix	5.583	5.081	5.332	0.502	0.91	0.05	14000	5300
-	Air-Mix	-	-	-	-	-	-	-	-
-	Air-He	-	-	-	-	-	-	-	-
N092	Air-He	3.203	3.340	3.272	-0.137	1.04	-0.02	8099	1086
N091	Air-He	3.093	3.411	3.252	-0.318	1.10	-0.05	7820	1110
N089	Air-He	5.655	5.601	5.628	0.054	0.99	0.00	14298	1822
N088	Air-He	5.510	5.826	5.668	-0.316	1.06	-0.03	13932	1895
N087	Air-He	5.290	6.091	5.691	-0.801	1.15	-0.07	13375	1981

†Note that a negative R represents shear with $u_2 > u_1$

†† $Re_{hc1(2)} = (\bar{u}_{1(2)} \cdot d_h)/\nu$ with the hydraulic half channel diameter $d_h = 40 \text{ mm}$

Table 2: *Experimental conditions for two mean velocities and three different stratification strengths.*

the centre and outer regions of the wake. As mixing progresses downstream, overall flow velocity is increased, as the boundary layer at the walls grows inwards towards the centre of the flow. Continuity of mass dictates that to compensate for the growing boundary layer of decreased velocity at the walls, the velocity at the centre of the flow must increase. In the $(\overline{u'u'})^{0.5}$ graph corresponding to the isokinetic experiment N075 (Figure 2), it can be seen that the higher velocity RMS fluctuations coincide with the area inside the wake. The area outside the wake has a uniform velocity and therefore a lower fluctuating RMS component; inside the wake there is a velocity gradient, which leads to a higher RMS velocity. In the shear mixing case displayed in Figure 3, a velocity deficiency can be seen in the region following the splitter plate. However in the shear mixing case, the flow follows a different pattern than the isokinetic case showed in Figure 2. In the shear mixing case illustrated in Figure 3, again a wake is initially formed in the area following the splitter plate. This wake is filled more quickly

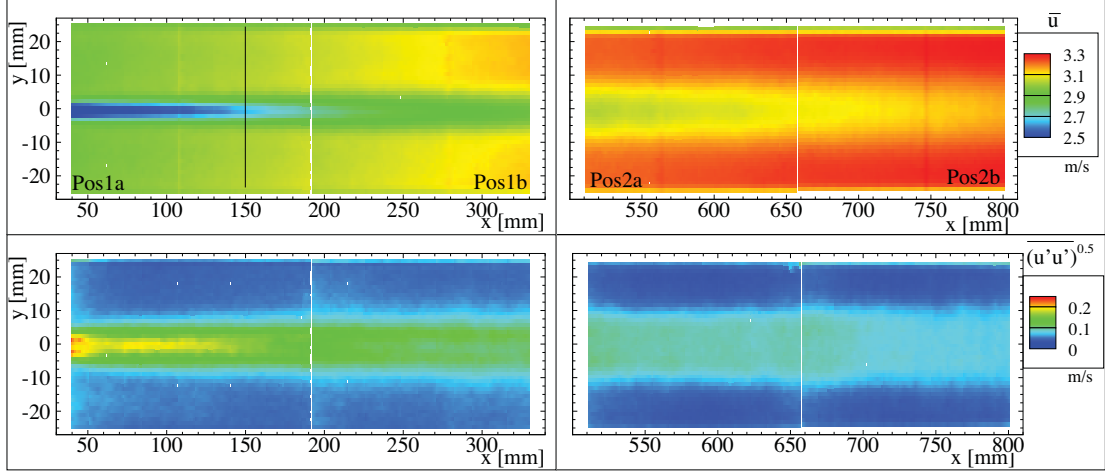


Figure 2: Mean velocity \bar{u} and velocity fluctuations $(\overline{u'u'})^{0.5}$ in stream wise direction recorded for experiment N075.

than the corresponding isokinetic case. As a consequence of friction, the mixing layer is deflected towards the low speed side. Finally, the velocity fluctuation $((u'u')^{0.5})$ graph shown in Figure 3 shows that the RMS fluctuations for the shear mixing case are far more spread out, in the crosswise direction for distances $x > 500 \text{ mm}$, than those in Figure 2, which are neatly contained in the area in close proximity to the isokinetic wake.

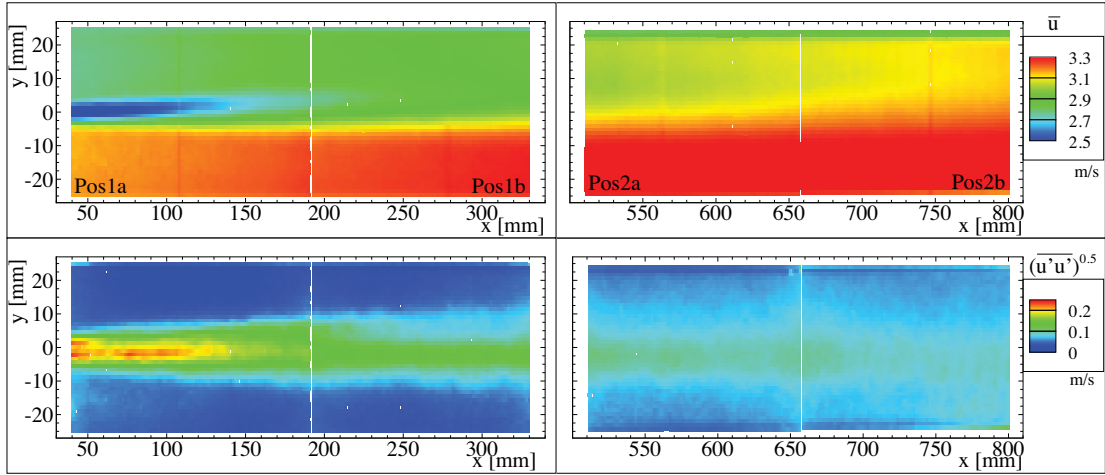


Figure 3: Mean velocity \bar{u} and velocity fluctuations $(\overline{u'u'})^{0.5}$ in stream wise direction recorded for experiment N077.

Some velocity statistics for the air-air mixing experiments N075, N076 and N077 are presented as line profiles extracted at positions $x = 150 \text{ mm}$ in Figure 4. In the isokinetic case (N075), the velocity profile is symmetric, with a velocity deficit at $y = 0$ corresponding to the splitter plate location.

As the shear is increased in experiments N076 and N077, this dip in velocity moves off centre, towards the upper (lower velocity) side. In the shear mixing cases, the

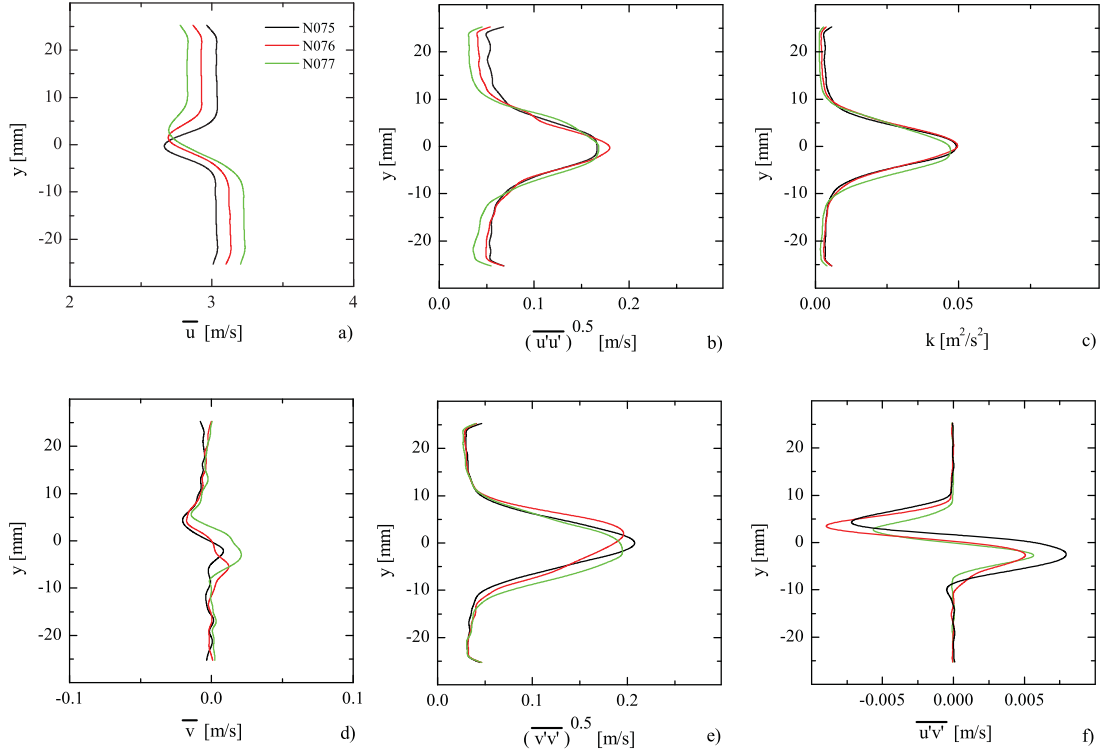


Figure 4: Comparison of statistical velocity quantities extracted along a vertical profile at $x = 150 \text{ mm}$ for experiments N075, N076 and N077.

friction between the two streams resultst in a deflection of the mixing zone towards the low velocity side accordingly, the dip in velocity is moved upwards into the slower velocity stream. For the corresponding RMS velocities $(\overline{u'u'})^{0.5}$ (Figure 4 b), the peak in the velocity fluctuations remains at $y = 0$, for all three experiments. The mean velocity in cross wise direction is close to zero except for the small part surrounding $y = 0 \text{ mm}$ (Figure 4 c). In this section, all experiments showed the same pattern of very low non-zero values, before returning back to zero. The shape of the $(\overline{v'v'})^{0.5}$ profile is similar to those for $(\overline{u'u'})^{0.5}$ (Figures 4 b versus c). For the turbulent kinetic energy k (Figure 4 e) we find low values in the outer part of the flow, with peaks for all experiments at approximately $0.05 \frac{m^2}{s^2}$ in the centre of the stream ($y = 0$). The isokinetic and shear trials (N075 versus N076 and N077) are nearly identical, with respect to the shape and peak value. This is a somewhat unexpected result; our expectation was to find a higher peak in the turbulent kinetic energy curve occurring in the shear flow experiments as a result of the velocity difference between the two streams which create a steeper velocity gradient and accordingly higher values of k . We expect that the high degree of similarity between the graphs is a result of the shear that is created from the velocity deficit in the centre of the wake; this shear is very strong such that the additional shear introduced by the velocity difference is not visible. In the future, it is suggested that experiments be conducted to examine the potential effects of shear strength on turbulent kinetic energy. The Reynolds' stress $\overline{u'v'}$ profile (Figure 4 f) is

zero outside the mixing zone, while the higher fluctuations corresponding to the region where k is also high.

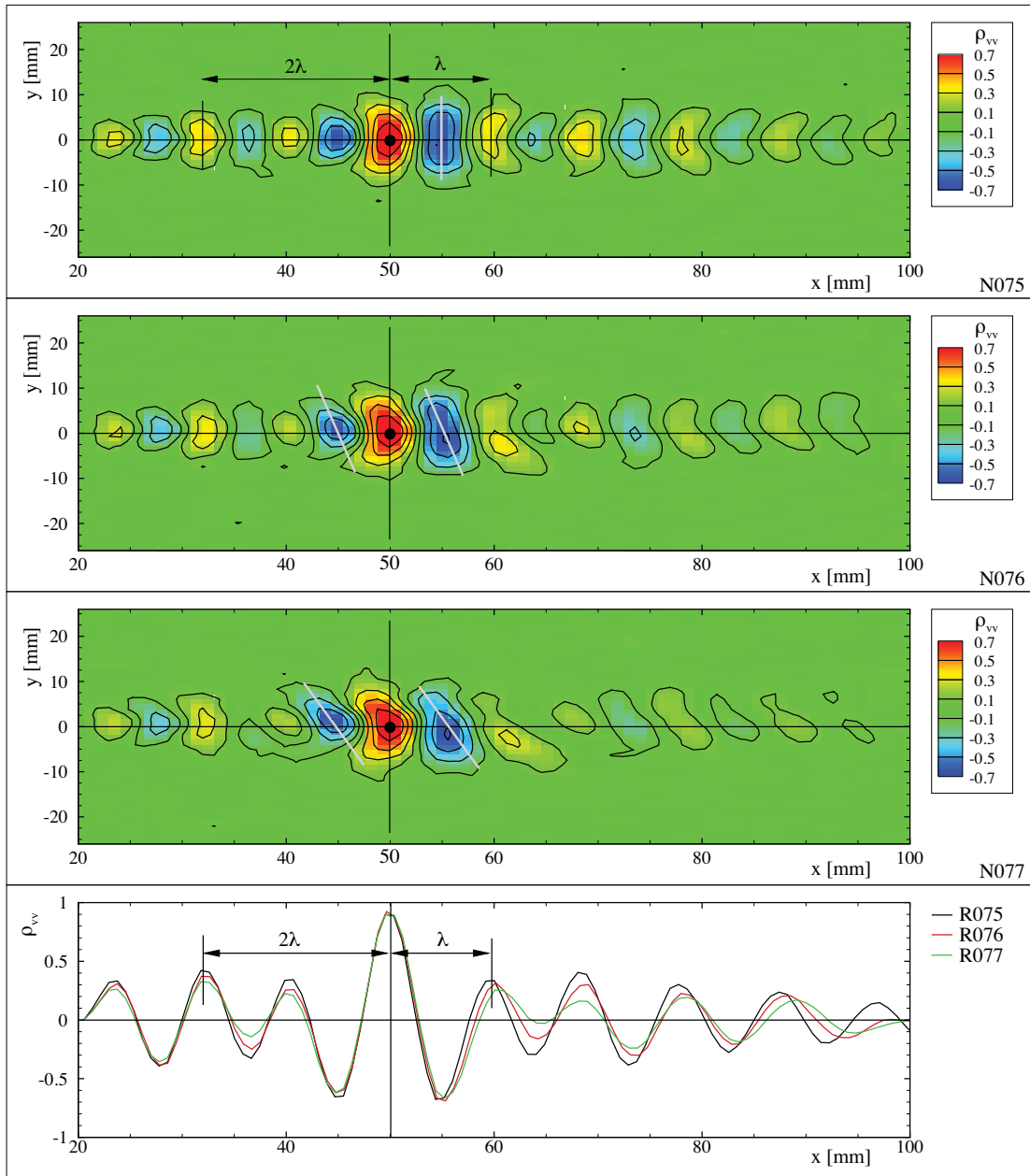


Figure 5: Normalized correlation maps of the transverse velocity v for experiments N075, N076 and N077 together with correlation profiles extracted at $y = 0$ mm.

The spatial cross-correlation maps $\rho_{vv}(x, y)$ for the velocity signals $v(x, y)$ with reference points at location $(50, 0)$ are presented in Figure 4 for experiments N075, N076 and N077 together with correlation functions extracted at $y = 0$. Iso-correlation contours were added to show the deformation of the correlated areas by the shear flow. All three experiments show a regular pattern of alternating positive and negative correlated areas which allow for the identification of the wavelength λ of the vortices

generated past the splitter plate tip. These vortices are convected approximately with the velocity \bar{u}_m which results in $f_n = \bar{u}_m/\lambda$ for the calculation of a characteristic frequency.

Defining a Strouhal number:

$$Str = \frac{f_n \delta_{m0}}{\bar{u}_m} \quad (1)$$

with the initial momentum thickness δ_{m0} of the boundary layer at the tip of the splitter plate, it is found that $Str = 0.046$ for turbulent boundary layers and $Str = 0.032$ for laminar boundary layers (Ho and Huerre (1984)). If we assume that the growth of the boundary layer on the splitter plate past the last grid on the high speed side follows the generalized law:

$$\delta_{m0} = A \cdot \left(\frac{\nu L}{\bar{u}_1} \right)^{1/2} \quad (2)$$

it follows with:

$$\bar{u}_1 = \bar{u}_m + \frac{\Delta \bar{u}}{2} = \bar{u}_m \left(1 + \frac{\Delta \bar{u}}{2\bar{u}_m} \right) = \bar{u}_m (1 + R) \quad (3)$$

together with eq. (1):

$$f_n = \underbrace{Str \cdot A^{-1} (1 + R)^{1/2}}_B \cdot \bar{u}_m^{3/2} \quad (4)$$

and therefore $f_n \sim \bar{u}_m^{3/2}$. To test this hypothesis, the natural frequencies as a function of mean velocities are presented in Figure 6 together with approximation functions $f_n = B \cdot \bar{u}_m^{3/2}$.

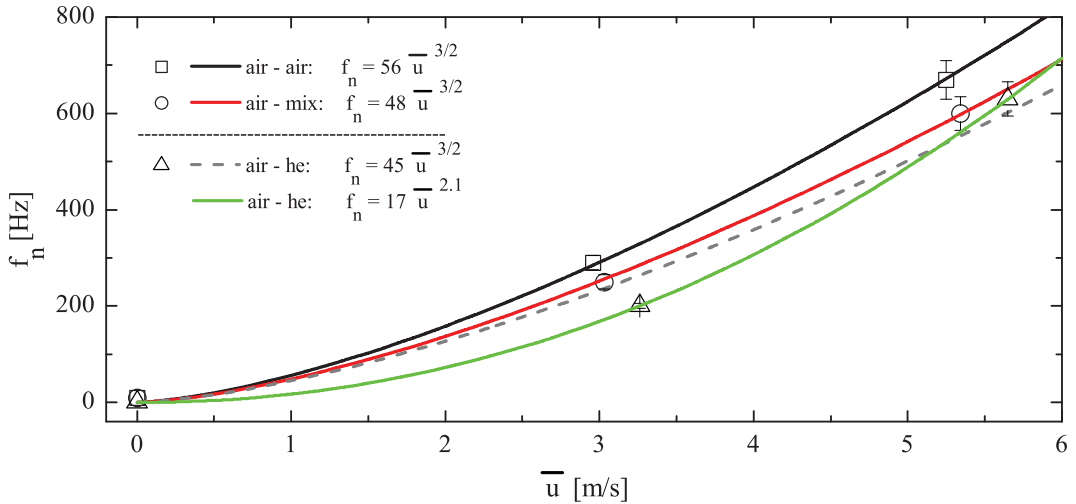


Figure 6: Natural frequency as a function of mean velocity together with approximation functions.

For the unstratified cases (N075-N080) as well as for the medium stratified experiments (N082-N086) we find a good agreement between the experiments and the relation $f_n \sim \bar{u}_m^{3/2}$ while for the strong stratification (N087-N092) there is considerable lack of

agreement. This disagreement might be caused by the state (laminar versus turbulent, see Tables 1 and 2) of the upper gas stream which is most probably laminar for the lower mean velocity case (N092 and N091) while it is turbulent for the unstratified case at both mean velocities and at least transitional for the medium stratification again for both mean velocities especially if one considers the disturbances introduced by the grids in the conditioning section. Therefore this effect requires a refined analysis which is beyond the scope of this paper.

4 Conclusions

Gas shear layers and wake flow experiments with different density stratifications were conducted in the HOMER facility consisting of a horizontal mixing section fed by two vertically stacked initially separated gas streams which interact downstream of a splitter plate. Three parameters were varied: (i) the mean velocity of the flow, (ii) the shear strength between the two streams and (iii) the stratification strength. For the unstratified experiments, first shear layer results demonstrate qualitatively the deflection of the developing flow field towards the low speed side while the flow field remains symmetric with respect to the test section top and bottom wall for the isokinetic case. For all experiments a vortex chain is formed past the splitter plate tip. These vortices were made visible with normalized cross-correlation maps ρ_{vv} based on the transverse velocity component. From the ρ_{vv} maps characteristic wavelengths λ_n and corresponding frequencies f_n of the vortices were calculated for all stratification strengths. The theoretical proportionality between the frequency and the mean velocity $f_n \sim \bar{u}_m^{3/2}$ was confirmed by all of the experiments except for the helium test cases at low velocities. The latter issue is attributed to the low Re number in the helium stream resulting in laminar flow conditions.

Acknowledgment

We would like to thank the staff member Willi Bissels for his engaged support in designing and manufacturing the experimental facility.

References

- Bell, J. H., Metha, R. D., Dec. 1990. Development of a two-stream mixing layer from tripped and untripped boundary layers. *AIAA Journal* 28 (12), 2034–2042.
- Bidokhti, A., Britter, R., 2002. A large stratified shear flow water channel facility. *Experiments in Fluids* 33 (2), 281–287.
- Bogdanoff, D. W., Nov. 1984. Interferometric measurement of heterogeneous shear-layer spreading rates. *AIAA Journal* 22 (11), 1550–1555.
- Browand, F. K., Latigo, B. O., 1978. Growth of the two-dimensional mixing layer from a turbulent and nonturbulent boundary layer. *Phys. Fluids* 22, pp. 1011–1019.
- Brown, G. L., Roshko, A., 7 1974. On density effects and large structure in turbulent mixing layers. *Journal of Fluid Mechanics* 64, 775–816.
- Dahm, W. J. A., Scheil, C. M., Tryggvason, G., 8 1989. Dynamics of vortex interaction with a density interface. *Journal of Fluid Mechanics* 205, 1–43.
URL 1
- Dimotakis, P. E., Nov. 1986. Two-dimensional shear-layer entrainment. *AIAA Journal* 24 (11), 1791–1796.
- Fernando, H. J. S., 1991. Turbulent mixing in stratified fluids. *Annual Review of Fluid Mechanics* 23 (1), 455–493.
- Fernando, H. J. S., Long, R. R., 2 1985. On the nature of the entrainment interface of a two-layer fluid subjected to zero-mean-shear turbulence. *Journal of Fluid Mechanics* 151, 21–53.
- Hill, J. A. F., Nicholson, J. E., 1964. Compressibility effects on fluid entrainment by turbulent mixing layers. Vol. 131. National Aeronautics and Space Administration.
- Ho, C.-M., Huerre, P., 1984. Perturbed free shear layers. *Ann. Rev. Fluid Mech.* 16, pp. 365–424.
- Johnson, D. A., 1971. An investigation of the turbulent mixing between two parallel gas streams of different composition and density with a laser doppler velocimeter. Ph.D. thesis, University of Missouri–Columbia.
- Konrad, J., 1977. An experimental investigation of mixing in two-dimensional turbulent shear flows with applications to diffusion-limited chemical reactions.
- Koochesfahani, M. M., Dimotakis, P. E., 9 1986. Mixing and chemical reactions in a turbulent liquid mixing layer. *Journal of Fluid Mechanics* 170, 83–112.
- Linden, P. F., 1975. The deepening of a mixed layer in a stratified fluid. *Journal of Fluid Mechanics Digital Archive* 71 (02), 385–405.
- McGrath, J. L., Fernando, H. J. S., Hunt, J. C. R., 9 1997. Turbulence, waves and mixing at shear-free density interfaces. part 2. laboratory experiments. *Journal of Fluid Mechanics* 347, 235–261.
- Mehta, R., Westphal, R., 1986. Near-field turbulence properties of single-and two-stream plane mixing layers. *Experiments in fluids* 4 (5), 257–266.
- Mory, M., 2 1991. A model of turbulent mixing across a density interface including the effect of rotation. *Journal of Fluid Mechanics* 223, 193–207.
- Rohr, J. J., Itsweire, E. C., Helland, K. N., Atta, C. W. V., 10 1988. Growth and decay of turbulence in a stably stratified shear flow. *Journal of Fluid Mechanics* 195, 77–111.
- Tavoularis, S., Corrsin, S., 3 1981. Experiments in nearly homogeneous turbulent shear flow with a uniform mean temperature gradient. part 2. the fine structure. *Journal of Fluid Mechanics* 104, 349–367.
- Veeravalli, S., Warhaft, Z., 7 1990. Thermal dispersion from a line source in the shearless turbulence mixing layer. *Journal of Fluid Mechanics* 216, 35–70.
- Yoon, K., Warhaft, Z., 6 1990. The evolution of grid-generated turbulence under conditions of stable thermal stratification. *Journal of Fluid Mechanics* 215, 601–638.